ELSEVIER

Journal of Photochemistry and Photobiology A: Chemistry 128 (1999) 39–45

Journal of Photochemistry and Photobiology A:Chemistry

www.elsevier.nl/locate/jphotochem

Spectroscopic studies of four new derivatives of benzamide

M. Brozis [a,*], J. Heldt [a], J.R. Heldt [b]

[a] *Institute of Physics, Pedagogical University Słupsk, 76-200 Słupsk, Poland*
[b] *Institute of Experimental Physics, University of Gdañsk, 80-952 Gdañsk, Poland*

Received 12 July 1999; accepted 15 July 1999

Abstract

Four new benzamide derivatives i.e. *N*-(4′-methyl)phenylbenzamide (I); *N,N*′-methyl(4′-methyl)phenylbenzamide (II); *N*-benzylbenzamide (III) and *N*-(4′-nitro)phenylbenzamide (IV) have been spectroscoply studied in hydrocarbon and weak polar solvents. The fluorescence studies show that some of those derivatives (I and II) in the excited state undergo conformation changes caused by proton transfer reaction or twisted intramolecular charge-transfer processes. Making use from the determined λ_{max} values of the absorption and fluorescence spectra the dipole moment of the molecules in the S_1 state has been evaluated for I, II and III. ©1999 Elsevier Science S.A. All rights reserved.

Keywords: Benzamide derivatives; Fluorescence spectra; Intramolecular charge-transfer

---

1. Introduction

Benzamides, under study, belong to the class of hetero-polar molecules in which chromophores are linked by a peptide bridge. For these molecules the peptide linkage plays a significant role of a ‘spacer’ between two molecular structures, the donor (D) and acceptor (A). Such molecules in the excited state undergo configuration changes: the donor moiety of benzanilide twist to a plane perpendicular with the plane describing the acceptor part of the molecule, causing an intramolecular electronic energy transfer between D and A. Thus, in the emission the normal F_1(LE) fluorescence, characteristic for the Franck-Condon structure of the S_0 state, is accompanied by another structureless F_2''(CT) emission. This emission takes place at energies lower than F_1(LE) and is originating from the excited state, S_1(CT), of a mutually perpendicular chromophore D^+ — A^- structure reached via the twisted intramolecular charge-transfer (TICT) process [1,2,3]. Tang et al. [4] have shown that for benzanilide dissolved in deairate hydrocarbon solvents the F_2 band is overlaid by an additional transition, F_2' (PT), originating from a *cis*-benzanilide tautomer founded in a doubly H-bonded dimer. The complicity of the F_2 band of benzanilide was confirmed by the dielectric solvents effects on spectral position, F_2 band half-width changes, chemical substitution and solvent environmental effects [2,3,5] as well as by time-resolved absorption spectroscopy and fluorescence decay studies [6].

In 1991, Azumaya et al. [7] in a very scrupulous work on the spectroscopic and fluorescence decay studies of 16 derivatives of benzanilide and *N*-methylbenzanilide with methyl group(s) ortho to the amide bond showed, that the amide bond must be rotated for the F_2 emission. The data indicate that the F_2 emission is mainly generated from excited twisted intramolecular charge-transfer (TICT) species with twisted amide bond.

In this paper, we report results of spectroscopic studies of four benzamide derivatives in which the methyl and nitro-functional groups are mezo substituted to the amide bond in the *N*-benzene ring. The chemical structures of the molecules under studies are given in Chart 1.The above functional groups with donating and withdrawing ability influence the amide bond and therefor the F_2 intensity as well. Additionally, to underline the importance of the amide bond rotation on the F_2 emission similar spectroscopic studies for *N*-benzylbenzamide (III) have been performed. In III the methylene group inserted between the *N*-phenyl and the peptide linkage change the length and flexibility of the ‘spacer’ between the donor and acceptor braking the conjugation between the A and D chromophore.

---

[*] Corresponding author.

1010-6030/99/$ – see front matter
PII: S1010-6030(99)00153-7

Chart. 1

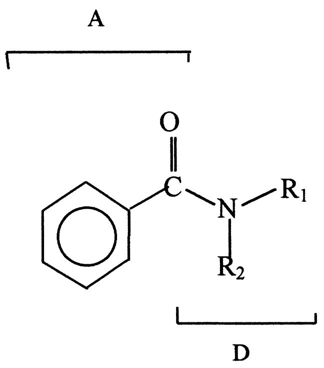

	R_1	R_2
I. *N*-(4'-methyl)phenylbenzamide	$-C_6H_4(CH_3)$	H
II. *N,N'*-methyl(4'-methyl) phenylbenzamide	$-C_6H_4(CH_3)$	CH_3
III. *N*-benzylbenzamide	$-(CH_2)C_6H_4(CH_3)$	H
IV. *N*-(4'-nitro)phenylbenzamide	$-C_6H_4(NO_2)$	H
Parent molecules		
benzamide	H	H
benzanilide	$-C_6H_5$	H

2. Experimental details

Benzanilide, methylcyclohexane (MCH), cyclohexane (CH), hexane (H), butyl ether (BE), ethyl ether (EE), ethyl acetate (EA) and tetrahydrofurane (THF) were purchased from Aldrich Chemical Co. The solvents MCH and CH were distilled before use from a sodium potassium amalgam, to ensure they are pure and free of water. The other solvents were distilled in the usual way, its purity have been checked by absorption and fluorescence method. Benzanilide and *N*-methylbenzanilide were twice recrystallized from methanol before use. The compounds I, II, III and IV were synthesized friendly by Rachoñ [8] and purified by recrystalization from methanol. The chemical structure as well as the purity of the compounds were tested by NMR spectra.

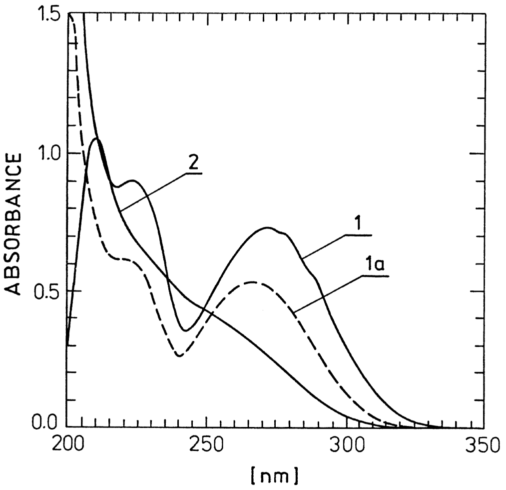

Fig. 1. The absorption spectrum of *N*-(4'-methyl)phenylbenzamide, I, curve (1) and *N,N'*-methyl(4'-methyl)phenylbenzamide, II, curve (2) in CH at 296 K. The absorption spectra of benzanilide (1a) is given for comparison.

Absorption spectra measurements were carried out using a Shimadzu UV-200 spectrophotometer. The luminescence spectra at 293 and 77 K were recorded on a Baird-Atomic (Model SFR-100) spectrofluorimeter using at low-temperature the sample compartment with a vacuum-sealed quartz cold finger dewar. The luminescence radiation was observed perpendicular to the direction of the excitation beam. For the measurements at 293 K, a sample was put into a standard rectangular Suprasil 10 mm cell, whereas at 77 K in a 2 mm diameter quartz tube placed in the dewar containing liquid nitrogen.

The concentration of solutions studied was about 5×10^{-4} M in all types of measurements. Molecule IV is not soluble in hydrocarbon solvents therefor its studies were performed in polar solvents only. The luminescence spectra have been corrected for the spectral response of the photomultiplier used.

3. Results and discussion

3.1. Absorption and luminescence spectra

Figs. 1 and 2 show the absorption spectra of compounds under studies. The absorption spectrum of I in MCH in the region of 200–350 nm consists two distinct bands: a strong band around 223 nm ($\varepsilon = 14{,}300\,M^{-1}\,cm^{-1}$) and another at 275 nm ($\varepsilon = 15{,}200\,M^{-1}\,cm^{-1}$). Similar as in benzamide we suppose the existence of a third, a very weak ($\varepsilon = 600\,M^{-1}\,cm^{-1}$) $n\pi^*$ absorption band at 295 nm. This band is overlapped by the second strong $\pi\pi^*$character band [3]. Its existence reveals the fluorescence excitation spectrum shown Fig. 3. Comparing the absorption spectrum of I with that of benzanilide (see Fig. 1) it follows, that the 275 nm band is shifted by 850 cm^{-1} to larger λ-values whereas the position of the 223 nm band is unchanged. The methyl group substituted at the 4 position of the *N*-phenyl ring increases the ε_M value of both absorption peaks by about 10%.

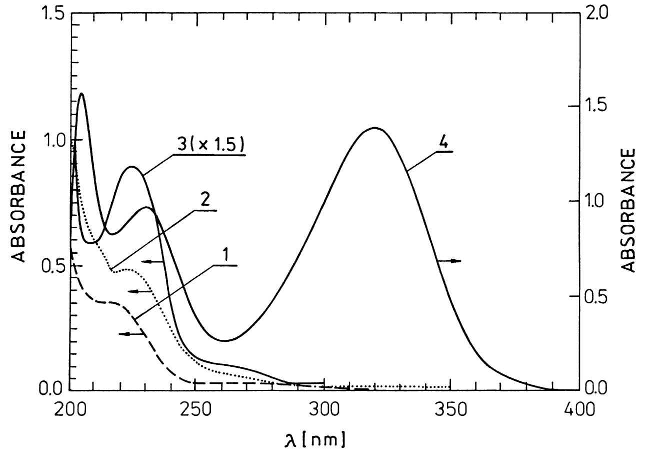

Fig. 2. Absorption spectra of *N*-benzylbenzamide, III, (curves: 1-vapor, 2-CH solution), and of *N*-(4′-nitro)phenylbenzamide, IV, (curve 4 in MeOH). The absorption spectrum of benzamide (curve 3) is given for comparison.

The $-CH_3$ group replacing the H atom at the nitrogen (see compound II) causes a drastic change in the absorption spectrum (see curve 2 in Fig. 1). The spectrum of II is understood if we found that the short wave band (at about 225 nm in I) is shifted to longer waves whereas the positions of the two other bands, i.e. 275 and 295 nm, remain unchanged. Also, this substituent leads to a decrease of the longwave band intensity contributing to the formation of an unstructured spectrum. The absorption spectrum of II is similar in shape to that of *N*-methylbenzanilide [3]. The absorption spectrum of II is shifted to longer wavelengths by 650 cm^{-1} in comparison to *N*-methylbenzanilide.

Fig. 2 shows the absorption spectra of molecules III and IV. Molecule III in CH solution has two bands: one at 228 nm ($\varepsilon = 11{,}000\,M^{-1}\,cm^{-1}$) and the other, which is very weak ($\varepsilon = 500\,M^{-1}\,cm^{-1}$), at about 275 nm. The existence of the last one is supported by the distinct maximum of the fluorescence excitation spectrum (see Fig. 4 curve 4). The absorption spectrum of III in the gas phase (curve 1 on Fig. 2) possesses the same shape but is shifted by about 600 cm^{-1} to smaller wavelength. On the same figure, the benzamide absorption spectrum is given for comparison. The absorption bands of this molecule appear at the same wavelength than that of III. It points out that the conjugation between A and D chromphoric group is destroyed by the $-CH_2$-bridging group additionally introduced between the peptide linkage and the *N*-phenyl substituent.

The nitro substituent in IV causes a large shift of the longwave maximum ($\lambda_{max} = 315$ nm versus 275 nm for I), and increases the molar absorption coefficient by about 65% ($\varepsilon_{315\,nm} = 24{,}600\,M^{-1}\,cm^{-1}$). This behavior is in agreement with observations of other authors [9] and theoretical predictions of Murrell [10]. It should be noted that the influence of the parent benzamide group is reduced compared to a regular mezo-substituent of nitrobenzene.

Figs. 3 and 4 show the fluorescence and fluorescence excitation spectra of the molecules under study. The fluorescence emission of I (see Fig. 3), as expected from the molecular structure, consist two bands: the normal fluorescence band F_1 (onset 310 nm $\lambda_{max} = 330$ nm in MCH solution) and the second more intense band F_2 (onset 400 nm $\lambda_{max} = 492$ nm). The F_2 band, if detected in hydrocarbon solutions, consists of two independent electronic transitions attributed to the proton-transfer imidole tautomer fluorescence $F'_2(PT)(S'_1(PT) \rightarrow S''_0(PT))$, and to the internal charge-transfer isomer fluorescence $F''_2(CT)((S''_1(CT) \rightarrow S''_0(FC))$. Fig. 3 shows also the $F'_2(PT)$ and $F''_2(CT)$ bands of I in MCH solution which result from decomposition of the

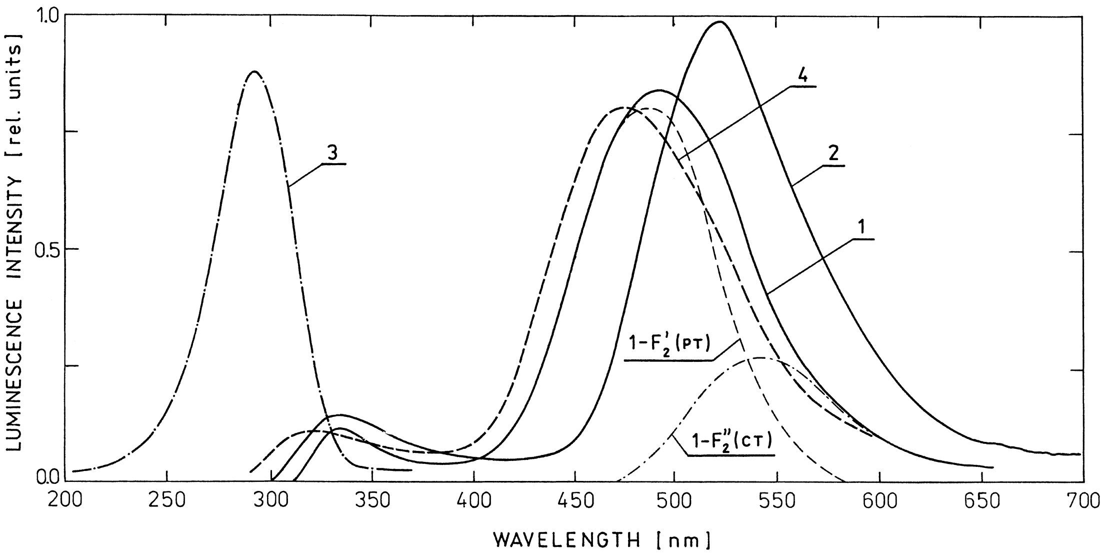

Fig. 3. Fluorescence spectrum of *N*-(4′-methyl)phenylbenzamide, I, (curve 1), *N,N*′-methyl(4′-methyl)benzamide, II, (curve 2) and fluorescence excitation spectrum (curve 3) of I in MCH solution at 293 K. The fluorescence spectrum of benzanilide (curve 4) in MCH is given for comparison only.

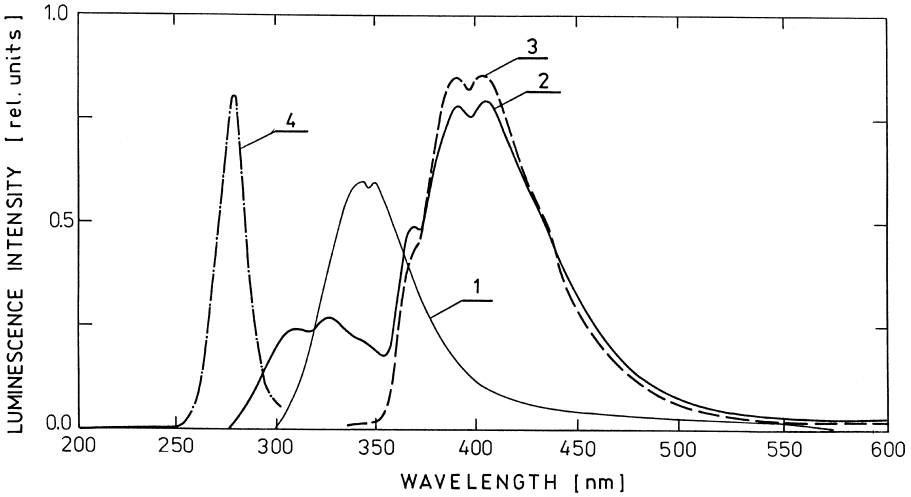

Fig. 4. *N*-benzylbenzamide (III) in EPA solution: (1) the fluorescence spectrum at 296 K, (2) the total luminescence (Fl + Ph) spectrum at 77 K, (3) the phosphorescence spectrum at 77 K, (4) the overlapping fluorescence and phosphorescence excitation spectra taken at 296 and 77 K.

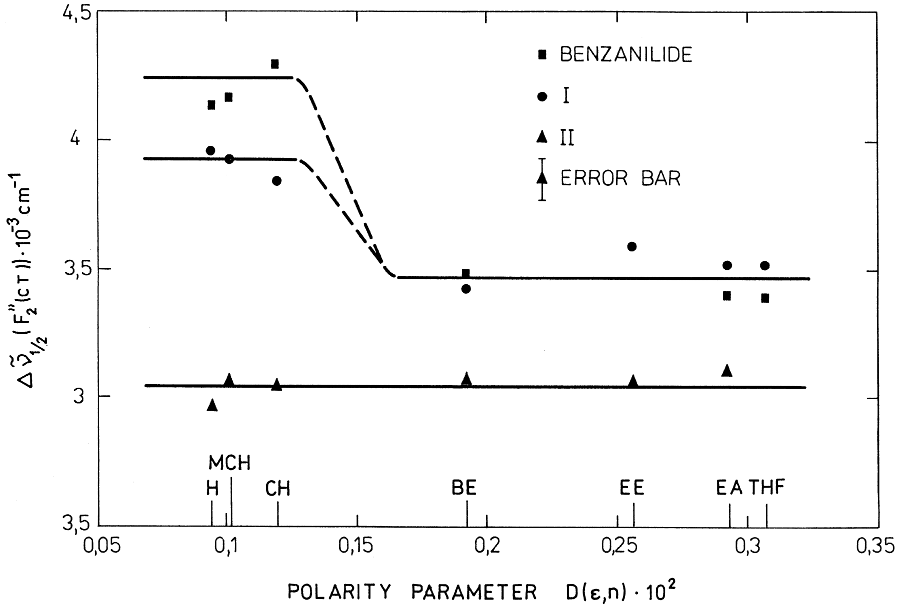

Fig. 5. The half width (FWHM) of the F_2 band of benzanilide, I and II vs. the Lippert $\Delta D(\varepsilon, n)$ function.

total emission into two bands of equal half-width (dashed curves with $\Delta\tilde{\nu}_{1/2} = 3300\,\mathrm{cm}^{-1}$). They participated in the total F_2 emission by about 75 and 25%.

The F_2 band complexity is clearly shown studying the dependence of the F_2 band half-width versus the Lippert $D(\varepsilon, n)$ function of the solvents used. This dependence, graphically presented in Fig. 5, shows a distinct change in the $\Delta\tilde{\nu}_{1/2}$ (F_2) value going from the hydrocarbon to the weak-polar solutions, i.e. $\Delta\tilde{\nu}_{1/2}$ (F_2) = 3960 cm^{-1} in H versus 3100cm^{-1} in EA.

From the view of the molecular structure the methyl-substituted compound, i.e. molecule II, can exhibit the F_1(LE) and the F_2''(CT) emission modes only. In Fig. 3 the curve 2 presents the fluorescence emission spectrum of molecule II. The spectrum possesses two bands: the F_1(LE) with $\lambda_{max} = 335$ nm and the F_2''(CT) with $\lambda_{max} = 521$ nm in MCH solution. The ratio of F_2/F_1 intensities for I and II depends on the kind of solvent, i.e. decreases with an increasing value of the dielectric constant. Here, it must be noted that the molecule I exhibit F_2'(PT) fluorescence only in hydrocarbon solvents, whereas the F_2''(CT) band is observed in all solvents used by us. The λ-values of the band maxima and its half widths are collected in Table 1. It can be seen that the half-width of molecule I is by about 300 cm^{-1} smaller than for II.

In Fig. 3 curve 3 shows the fluorescence excitation spectrum of I. This spectrum possesses one peak with λ_{max} at 295 nm. According to the quantum mechanical calculation

Table 1
The lang wave absorption and emission band maxima $\tilde{\nu}$ (in cm^{-1}), the radius of Onsager cavity a_0(in 10^{-10} m), the permanent dipole moments (in Debye) of the ground, μ_g, and excited μ_{ex} states of the benzamide derivatives and half-width of the F_2''(CT) band

Number	Compound	Solvent	Polarity parameter $D(\times 10^{-2})$	$\tilde{\nu}_{em}$	$\tilde{\nu}_{abs}$	$\tilde{\nu}_{abs} - \tilde{\nu}_{em}$	$\Delta\tilde{\nu}_{1/2}(F_2'')$	Onsager cavity radius a_o	Dipole μ_g	Moment μ_{ex}
0	*N*-phenyl-benzamide	H	0.096	20848	37450	16602	4130	2.80[a]	3.66[c]	**8.86**
		MCH	0.101	20973	37400	16427	4161			7.91[a]
		CH	0.120	21053	37523	16351	4308			9.2[c]
		BE	0.192	19665	38314	17635	3421			
		EE	0.256	19585	37736	18729	3490			
		EA	0.293	18297	37023	18826	3514			
		THF	0.308	19305	37383	18678	3517			
I	*N*-(4′-methyl)-phenyl-benzamide	H	0.096	20292	36820	16528	3960	2.92[a]	3.80[d]	**8.36**
		MCH	0.101	20243	36750	16507	3925			9.25[a]
		CH	0.120	20313	36710	16397	3838			
		BE	0.192	19978	36820	17342	3485			
		EE	0.256	19420	36830	17410	3210			
		EA	0.293	19073	36846	17750	3270			
		THF	0.308	19120	36950	17830	3385			
II	*N*′*N*′-methyl-(4′-methyl)-phenyl-benzamide	H	0.096	19198			2962	3.11[b]	**3.91**[b]	**8.40**[f]
		MCH	0.101	19205			3064			
		CH	0.120	19164			3041			
		BE	0.192	18776			3069			
		EE	0.256	18454			3062			
III	*N*-benzylbenzamide	Vapour				45455		3.13[b]	**3.94**[b]	**6.28**[e]
		CH				44642				

[a] From [15].
[b] Calculated using HyperChem.
[c] From [11].
[d] From [16].
[e] Bold letter is our data determined using the $\tilde{\nu}_G$,$\tilde{\nu}_S$ values of the gas phase and CH solution absorption spectra [13].
[f] Since the absorption spectrum of II is unstructure we put the $\tilde{\nu}$(abs) = 0 in Eq. (1).

of Belotsvetov et al. [11] it corresponds to the very weak $n\pi^*$ absorption band which is baried in the very strong $S_1(\pi\pi^*) \leftarrow S_0$ absorption with $\lambda_{max} \sim 275$ nm. The fluorescence excitation spectrum of II overlaps that of I and for this reason it is omitted in Fig. 3. Comparing the emission spectra of I and II with that of benzanilide [12] it results, that they are similar in shape, but both are shifted to larger wavelengths, i.e. by 800 and 1850 cm^{-1}, respectively.

Molecule III in EPA solution shows a very weak fluorescence observed in the region 300–450 nm (Fig. 4, curve 1) which arises from a weak absorption band corresponding to excitation in a locally excited moiety i.e. benzamide. This is supported by the likewise absorption band contours to benzamide (see Fig. 2, curve 2 and 3). Molecule IV at room temperature in EPA and THF solutions does not show fluorescence. At 77 K a weak F_1(LE) emission is recorded. This spectrum is a mirror image of the absorption and excitation spectra.

The molecules under study at 77 K show more intense fluorescence emission than at 293 K. Beside the F_1(LE) band I and II show phosphorescence emission and a weak emission from the TICT isomer. Fig. 6 shows the total luminescence (Fl + Ph) spectrum of I in rigid solution of MCH and EPA mixture at 77 K. From the Figure it is evident that the total luminescence intensity curves possesses two bands. The emission in the region 300–350 nm is assigned as a F_1(LE) band, where as the strong band in the region 400–600 nm comprehends the phosphorescence and the F_2''(CT) emission. The band contours of the respective emission modes are labeled by (1) and (2). It must be pointed out that long-wavelength bands in the total emission spectra (heavy lines) of I and II differ from those of the pure

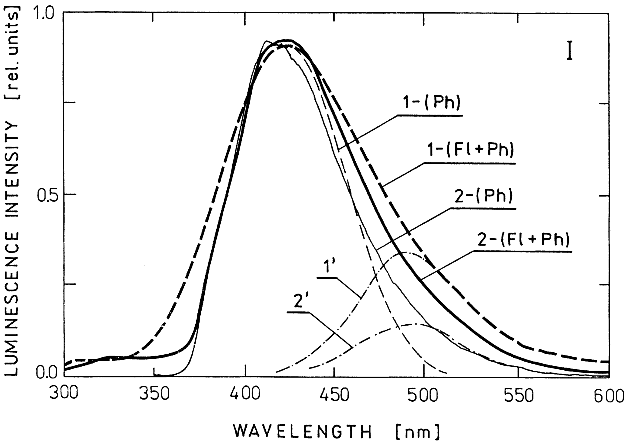

Fig. 6. The total emission (Fl + Ph) spectra of I in MCH (curve 1), in EPA mixture (curve 2) and pure phosphorescence (thin line) spectrum in EPA at 77 K. The dashed doted line 1′ and 2′ results from subtraction: 1-(Fl + Ph)−1-(Ph) and 2-(Fl + Ph)−2-(Ph), respectively.

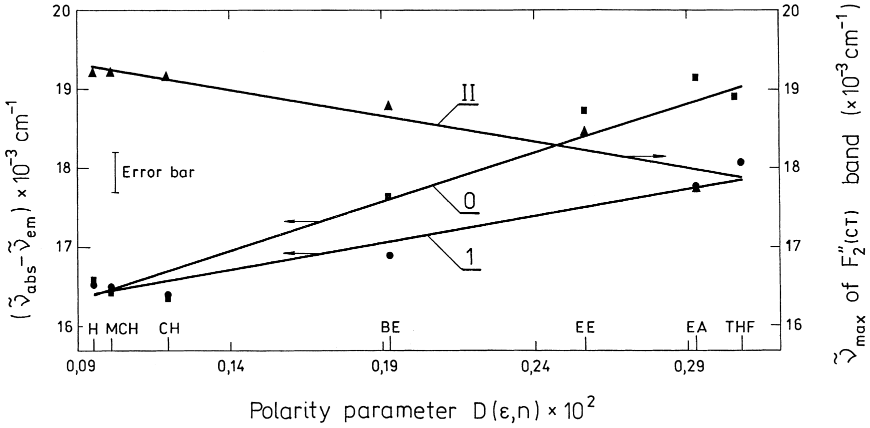

Fig. 7. The $\tilde{\nu}_{max}$(abs) − $\tilde{\nu}_{max}$(F_2) changes vs. the $\Delta D(\varepsilon, n)$ function of solvents used.

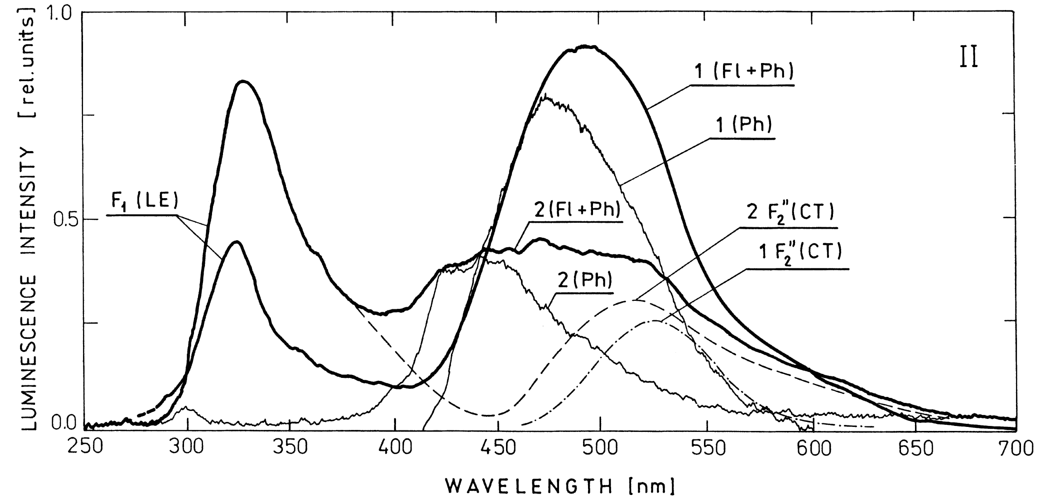

Fig. 8. The total emission (Fl + Ph) spectra of II in MCH (curve 1) and EPA mixture (curve 2) and corresponding phosphorescence spectra at 77 K. The dashed and dashed-doted lines are obtained from subtraction: 2-(Fl + Ph)−2-(Ph) and 1-(Fl + Ph)−1-(Ph), respectively.

phosphorescence spectrum (thin lines). Moreover, the F_2 fluorescence bands of these two compounds at 293 K show an anomaly i.e. the F_2 band has its maximum at larger wavelength than the phosphorescence band λ_{max} (F_2) > λ_{max} (Ph), (compare Fig. 3 with 4 and 6). Its is also distinctive, that in the EPA and MCH rigid solutions for I and II $\lambda_{max}(F_2 + \text{Ph}) > \lambda_{max}(\text{Ph})$. Such wavelength dependence is comprehensible if one assumes that at 77 K the band comprise an intense phosphorescence band and a weak F_2''(CT) band (Fig. 8). The 1' and 2' curves in Fig. 6 give the result of subtraction of the normalized phosphorescence spectra from the total luminescence spectra. This procedure gives a band which λ_{max} is in good agreement with that determined for the F_2''(CT) band at 296 K.

3.2. Solvent effect

As it has been mentioned, the absorption and fluorescence spectra of I and II as well as the parent molecule benzanilide were taken in solvents of different polarities. Determining the difference $\Delta\tilde{\nu}_{max} = \tilde{\nu}_{ab} - \tilde{\nu}_{em}$ between the maxima of the longwave absorption and fluorescence bands as a function of the solvent polarity the change of the permanent dipole moment of the molecules in the excited state have been evaluated. The values $\tilde{\nu}_{max}$ of the absorption and fluorescence bands and the Lippert's polarity function are collected in Table 1 and graphically presented in Fig. 7. As can be seen from the Figure a good linear plot is obtained with correlation factors $R = 0.92$, 0.98 and 0.96 for benzanilide, molecule I and II, respectively. Using the relation obtained by Liptay [14] Mataga and Kubota [15]

$$\Delta\tilde{\nu}_{max} = \tilde{\nu}(\text{abs}) - \nu[F_2''(\text{CT})] = \frac{2(\mu_{ex} - \mu_g)^2}{\text{hc}a_0^3} D(\varepsilon, n) \quad (1)$$

the dipole moment, μ_{ex}, of the molecules under study in the excited state was calculated. In (1) μ_g and μ_{ex} refer to the dipole moments of the ground and excited states of the molecule, a_0 is the radius of the Onsager cavity which fits the molecule (was calculated using the Hyperchem program) and

$$D(\varepsilon, n) = \frac{\varepsilon - 1}{2\varepsilon + 1} - \frac{n^2 - 1}{2n^2 + 1} \qquad (2)$$

where ε and n are the bulk solvent permittivity and the refractive index, respectively.

As can be seen from Fig. 7 the variation in the $\Delta\tilde{\nu}_{\max}$ value is rather large, ca. 2000 cm^{-1} versus $\Delta D(\varepsilon, n) = 0.21 \times 10^{-2}$ from hexane to the tetrahydrofurane. It indicates a reasonable big change in dipole moment of molecules under study in the excited state. The determined data are collected in Table 1 column 9. Comparing the μ_{ex} values for benzanilide and molecule I obtained by using the method of solvent induced shifts of electronic absorption bands [13] with that determined now a difference is noted. The difference equals 0.97 and 0.72 for benzanilide and I, respectively. The μ_{ex} value of benzanilide obtained in this work agrees good with the theoretical result of Belotsvetov et al. [11]. The noted differences in the μ_{ex} values obtained in [13] and now are comprehensible since they refer to the molecule structure of the ground and TICT excited states. The μ_{ex} value of III is equal to that of benzamide [13] i.e. 6.29 D for III and 6.33 D for benzamide. This result confirms that the benzamide moiety of III is responsible for the fluorescence emission. The μ_{ex} data of II and III are determined for the first time.

4. Conclusion

The fluorescence spectra of I and II obtained at room and low temperatures consist of two bands, the normal fluorescence band, $\lambda_{\max}(F_1) \sim 320$ nm, and a TICT isomer fluorescence emission at $\lambda_{\max}(F_2) \cong 500$ nm. The relative intensities of these bands depend on the solvent polarity. At 77 K both molecules in polar solution exhibit phosphorescence emission with $\lambda_{\max} \cong 420$ nm.

The molecules III and IV in EPA rigid solvent at 77 show fluorescence emission but only molecule III exhibit the phosphorescence. The fluorescence and phosphorescence spectra at 77 K show signs of vibration structure in polar solvent, (Fig. 8).

For molecules I, II and III the permanent dipole moment of the first singlet excited state has been determined using the solvent induced shifts of the absorption and fluorescence bands. They are calculated using the $\tilde{\nu}_{\max}$ values of the long-wave absorption band and F_2''(CT) band. As it has been said the F_2''(CT) band originates from the TICT isomer. Thus the μ_{ex} data determined in this work proceed to it.

Acknowledgements

The authors like to acknowledge financial support from the Pedagogical University of Słupsk and University of Gdañsk grant BW 5200-5-0282-9. J.H. is thankful to the Humboldt Foundation for the fellowship.

References

[1] W. Rettig, Angew. Chem. Int. Ed. Engl. 25 (1986) 4971.
[2] J. Heldt, D. Gormin, M. Kasha, Chem. Phys. 136 (1989) 321.
[3] J. Heldt, D. Gormin, M. Kasha, J. Am. Chem. Soc. 110 (1988) 8256.
[4] G.Q. Tang, J.M. MacInnis, M. Kasha, J. Am. Chem. Soc. 109 (1987) 2531.
[5] J. Heldt, M. Kasha, J. Mol. Liquids 41 (1988) 305.
[6] J. Heldt, J.R. Heldt, J. Kamiñski, Z. Naturforsch, in Print.
[7] I. Azumaya, H. Kogechika, Y. Fujiwara, M. Itoh, K. Yamaquchi, K. Shudo, J. Am. Chem. Soc. 113 (1991) 2833.
[8] J. Rachon, paper ready for publication.
[9] N.T. Turro, Modern Molecular Photochemistry, Chap. 13, Benjamin/Cunmings, Menlo Park, CA, 1978.
[10] J.N. Murrell, The Theory of the Electronic Spectra of Organic Molecules, Chap. 10, Wiley, New York, 1963.
[11] A.V. Belotsvetov, V.I. Danielova, E.V. Borisov, M.K. Verzilina, T.A. Saveleva, L.V. Gorchakov, Zhurnal. Fizicheskoi Khimii 50 (1976) 1941.
[12] J. Heldt, J.R. Heldt, E. Szatan, J. Photochem. Photobiol. A: Chem. 121 (1999) 91.
[13] J. Heldt, J.R. Heldt, M. Raciniewska, Z. Naturforsch 53(a) (1998) 684–688.
[14] W. Liptay, Z. Naturforsch. 20(a) (1965) 1441.
[15] N. Mataga, T. Kubota, Molecular Interactions and Electronic Spectra, Marcel Dekker, New York, 1970.
[16] L. McClellan, Tables of Experimental Dipole Moments, vol. 3, Rahara Enterprise, 1969.